Key Engineering Materials
ISSN: 1662-9795, Vol. 897, pp 39-44
doi:10.4028/www.scientific.net/KEM.897.39

Submitted: 2021-05-03
Accepted: 2021-05-06
Online: 2021-08-17

Aqueous Stability of Cross-Linked Thermal Responsive Tissue Engineering Scaffold Produced by Electrospinning Technique

YONG Hsin Nam Ernest[a], TSHAI Kim Yeow[b] and LIM Siew Shee[c]

Faculty of Science and Engineering, University of Nottingham Malaysia, Jalan Broga, 43500 Semenyih, Selangor, Malaysia

[a]kedy4yhr@nottingham.edu.my, [b]kim-yeow.tshai@nottingham.edu.my, [c]siewshee.lim@nottingham.edu.my

Keywords: PNIPAm, electrospinning, OpePOSS, tissue engineering, scaffold, nanofibers.

Abstract. Poly(N-isopropylacrylamide) (PNIPAm) has been one of the most widely studied thermal-responsive polymer in tissue engineering owing to its reversible hydrophilic-hydrophobic phase transition across its lower critical solution temperature (~32°C) that is close to human physiological temperatures. Among tissue engineering constructs, nanofibrous scaffolds offer an added advantage in mimicking the morphology of the native extracellular matrix (ECM). Electrospinning has been reported as one of the most facile method to produce PNIPAm nanofibres and neat electrospun nanofibres scaffold is known to possess poor aqueous stability, limiting its use in tissue engineering applications. In contrast, numerous studies on PNIPAm hydrogels have shown relatively good aqueous stability owing to the hydrophilic 3D crosslinked structure of the hydrogel which resist instant dissolution but rather swell to a greater or lesser extent. However, the presence of crosslinkages in PNIPAm hydrogels causes it to be hardly electrospinnable into nanofibres. In the present work, crosslinker free PNIPAm was radical polymerized to a high molecular weight of 385 kDa. To produce nanofibers, electrospinning was carried out on a dedicated %wt of PNIPAm solution containing octaglycidyl polyhedral oligomeric silsesquioxane (OpePOSS) and 2-ethyl-4-methylimidazole (EMI). Resulting PNIPAm nanofibrous network was found to strongly resemble the ECM morphology with fiber diameter of 436.35 ± 187.04 nm, pore size 1.24 ± 1.27 μm and 63.6% total porosity. Aqueous stability was studied in cell culture media over the course of 28 days. The current result shows significant improvement with a gradual mass loss up to a maximum of 35% instead of the near immediate dissolution observed in the case of electrospun neat PNIPAm scaffold without crosslinks.

Introduction

Tissue engineering is an interdisciplinary field that aims to restore, maintain or improve tissue functions by development of biological substitutes [1]. Deterioration and damage of tissues arising from diseases and injuries entail the need for conventional tissue autoplasty or transplant. However, these costly surgical treatments have significant drawbacks such as pain, discomfort, anatomical constraints, probable immune response due to tissue rejection, donor-patient disease introduction, infection and hematoma. Therefore, tissue engineering aims to regenerate tissues both in vitro and in vivo, mainly by utilizing porous constructs as tissue engineering scaffolds (TES) [2]. The major function of scaffolds is to provide mechanical support for adherent cells, and often designed to mimic the native extracellular matrix (ECM) to promote cellular activity. A fundamental criterion to a viable TES is the biocompatibility of the base material.

In such instance, thermally responsive poly(N-isopropylacrylamide) (PNIPAm) offers potential in tissue engineering applications owing to its inherent biocompatibility tested with various cell lines [3, 4]. It exhibits a reversible phase transition from hydrophilic to hydrophobic phases across its lower critical solution temperature (LCST) of ~32°C. Above its LCST, PNIPAm supports protein adsorption, cell adhesion and proliferation in its moderately hydrophobic state whereas below its LCST, the polymer is hydrated and hydrophilic interaction dominated bulk hydration of PNIPAm materials could induce cell release [4]. These conformational changes enable a spontaneous cell

harvesting mechanism while allowing operation within reasonable temperatures that are friendly to cells owing to the proximity of its LCST to the physiological temperature [5].

Electrospinning is one of the most attractive TES fabrication techniques attributable to its relative simplicity, reproducibility and cost-effectiveness in fabricating nanofibrous scaffolds from polymers that could highly mimic the structure of the ECM [6, 7]. Despite the potency of PNIPAm in many applications [4], electrospinning of the polymer has not been widely explored as evidenced from its limited publications.

In the authors' earlier work (unreported), neat un-crosslinked electrospun PNIPAm membranes exhibit poor stability in aqueous environment thus inhibiting its long-term usage for cell culture. Radical chain polymerization of NIPAm monomers in the presence of the bifunctional cross-linker N,N'-methylenebisacrylamide (BIS) yields crosslinked PNIPAm hydrogels that have been widely reported to be relatively stable in aqueous environments [8-11]. However, attempts to electrospin polymer solution containing PNIPAm hydrogels failed to yield consistent nanofibers, fibre diameter and distribution [12]. Wang et. al. related the poor electrospinnability to the insoluble nature of PNIPAm hydrogels [13], attributable to the 3D crosslinked architecture which reduce chain mobility and stretchability during electrospinning. In this work, in order to obtain an aqueous stable electrospun PNIPAm nanofibrous scaffold, cross-linking was performed post electrospinning and the degradation profile in aqueous environment was investigated.

Experimental

Materials. 97% NIPAm monomer, potassium persulfate (KPS), 99% sodium dodecyl sulfate (SDS) surfactant, dialysis tubes with molecular weight cut-off at 12 kDa, 95% EMI and HPLC grade methanol were purchased from Sigma-Aldrich. 99% THF and 99.9% DMF were purchased from Chemiz (M) Sdn. Bhd. OpePOSS was purchased from Hybrid Plastics Inc., Glasgow's minimum essential medium (GMEM) was purchased from Thermo Fisher Scientific. NIPAm was recrystallized once in n-hexane. All other chemicals were used as received.

PNIPAm Synthesis. PNIPAm was synthesised via radical polymerization from its monomer NIPAm in a 2-L cylindrical jacketed reactor (150 mm internal diameter fitted with an anchor type impeller of 90 mm diameter). 2 g of recrystallized NIPAm and 0.08 g (4 % (w/w) to monomer) of SDS were dissolved in 200 mL of distilled water (pH 5) in a beaker. The mixture was transferred into the jacketed reactor and adjusted to 80 ˚C. Concurrent bubbling with nitrogen gas to purge out oxygen was carried out for 20 min. Next, 0.02 g (1 % (w/w) to monomer) of KPS dissolved in 5 mL of distilled water was added to the mixture to initiate polymerization and purging with nitrogen was stopped. Stirring speed was held constant at 100 rpm and the mixture polymerized for the duration of 4 h. Right after polymerization, the cloudy mixture was transferred into a beaker and immediately quenched in a water bath at room temperature for 30 min, followed by dialysis against distilled water for 3 days (water refreshed twice daily). After dialysis, the solution was left in a −20 °C freezer for 24 h and lyophilized for 48 h at −59 °C and 0.012 mbar. The resulting wool-like dried samples were kept in tightly sealed containers until further processing and characterization.

PNIPAm Functional Group Analysis. Functional group analysis to confirm the synthesis of PNIPAm was conducted using Fourier transform infrared spectroscopy (FTIR) (Perkin Elmer Frontier FT-IR/FIR, USA). The analysis was conducted in attenuated total reflectance mode across 16 scans in the wavenumber range of 400 to 4000 cm^{-1}.

Molecular Weight Determination. The molecular weight of the synthesised PNIPAm was determined by static light scattering (SLS) (Malvern Panalytical Zetasizer Nano ZS, UK) with HPLC grade methanol as diluent and scattering standard. Dynamic light scattering was simultaneously run to insure sample stability. The differential refractive index increment (dn/dc) was determined to be 0.2021 ml/g over a set of concentrations of the synthesised PNIPAm in HPLC grade methanol and refractive index at each concentration was determined using refractometer (Atago 1T, Japan).

Preparation of Electrospinning Solution. Polymer solution for electrospinning was prepared with 15% (w/w) synthesised PNIPAm dissolved in THF:DMF (1:1). OpePOSS at 20% (w/w) and

EMI at 0.3% (w/w) in respect to weight of PNIPAm were added and continuously stirred for 1 h at room temperature to obtain a homogenous mixture.

Electrospinning of PNIPAm. The polymer solution was transferred into a glass syringe fitted with a G20 blunt spinneret. Feed rate was maintained at 0.6 ml/h by a syringe pump (New Era NE300, USA). Voltage was set to 9 kV (Gamma High Voltage, USA) and distance to grounded collector was 18 cm. Aluminum foil covered square acrylic plate (11cm × 11cm) was used as the collector. Ambient conditions were recorded at 55% relative humidity and temperature of 25°C. Electrospun nanofibrous scaffold was conditioned in a preheated oven maintained at 120°C for 4 h to allow for cross-linking. The crosslinked sample was stored in an airtight container containing silica gel until further use. Herein, electrospun PNIPAm membrane is referred to as esPNIPAm.

Morphology. Morphology of esPNIPAm was captured under a field emission scanning electron microscope (FESEM) (FESEM & EDX Quanta 400F, USA). Average fiber diameter and pore size distributions were analysed based on the SEM micrograph using ImageJ. Average fiber diameter and its distribution were obtained over 100 measurements with the 'measure' function while the average pore size and its distribution were obtained with the 'analyze particle' function that gives approximately 840 pores.

Porosity. Porosity of esPNIPAm was estimated using gravimetric method by determining the apparent and bulk density of the scaffold. Cross-sectional thickness of esPNIPAm was measured under FESEM, while the width and length were measured by a vernier caliper. Mass of the esPNIPAm sample was obtained using a microbalance (Mettler Toledo XP6, USA). The resulting apparent density was computed according to the relationship shown in Eq. 1. Total porosity of esPNIPAm was determined by Eq. 2., where NFM stands for nanofiber membrane.

$$\text{NFM apparent density} = \text{NFM mass} / \text{NFM volume}. \quad (1)$$

$$\text{Porosity} = 1 - (\text{NFM apparent density} / \text{polymer bulk density}). \quad (2)$$

Aqueous Stability. The aqueous stability of esPNIPAm was investigated by immersing esPNIPAm in GMEM incubated at 37°C and 5% CO_2. Percentage mass loss was determined over periods of 1, 2, 3, 5, 7, 14, 21 and 28 days. Pre-cut samples of esPNIPAm were weighed with a microbalance (Mettler Toledo XP6, USA) to a precision of 0.001 mg and initial weights were recorded. Final weights across different days of immersion were obtained by firstly removing respective samples, dried for two days in vacuum (300 mbar) at 40°C, and weighed. The percentage mass loss was computed according to Eq. 3 and the study was conducted in triplicates (n=3).

$$\%\ \text{mass loss} = [\ (\text{initial mass} - \text{final mass}) / \text{initial mass}\ ] \times 100\% \quad (3)$$

Results and Discussion

Functional Group Analysis. The characteristic functional groups of the synthesised PNIPAm was confirmed by FTIR spectroscopy. The FTIR spectrum (Fig. 1) shows conformance with PNIPAm reported in the literature [14]. The peaks at wavenumbers 2970 and 2931 cm^{-1} are assigned to the asymmetric stretch vibration of the isopropyl -CH_3 and the main backbone -CH_2, respectively. In the fingerprint region between 1627 and 1386 cm^{-1}, four characteristic peaks unique to PNIPAm, namely 1627, 1539, 1457 and 1386 cm^{-1} can be assigned to amide I, amide II, asymmetric deformation of isopropyl -CH_3 vibration and deformation of isopropyl -CH_3, respectively.

Molecular Weight of PNIPAm. Fig. 2 shows the Debye plot of the synthesised PNIPAm. The molecular weight was computed as 385 kDa by taking the inverse of the y-intercept. The second virial coefficient, A_2 of a polymer in a solution can be related to the strength of particle interaction and sample solubility [15]. A_2 was computed from the slope of the Debye plot as -4×10^{-4} ml mol/g^2 following the correlation in Eq. 4. The slight negative value suggests a mild agglomeration tendency of PNIPAm.

$$A_2 = \text{gradient of the Debye plot} / [(2)(1000)]. \quad (4)$$

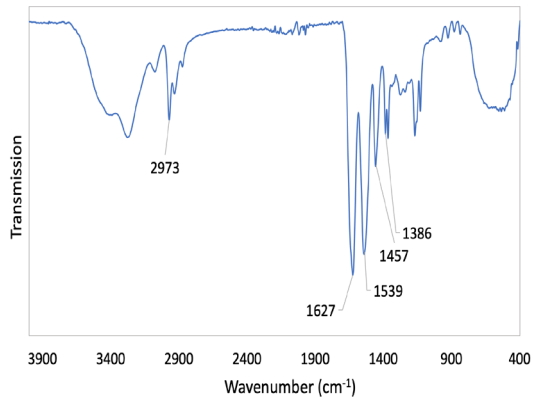

Figure 1. FTIR spectrum of the synthesised PNIPAm.

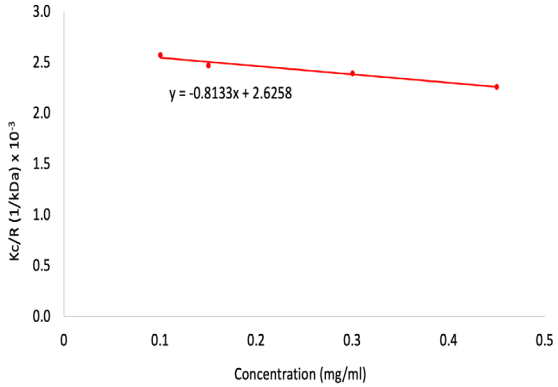

Figure 2. Debye plot of synthesised PNIPAm.

Morphology of esPNIPAm. Fig. 3 (a) and (b) shown uniform nanofibrous morphology and cross-section of esPNIPAm, respectively, under FESEM. The fiber diameter distribution is presented in Fig. 4 with a mean fiber diameter of 436.35 ± 187.04 nm. Overall fibers distribution is in the range from 100 to 1000 nm with relatively high proportion concentrated in the range of 200 to 700 nm. These indicate that the esPNIPAm highly mimics the fiber size of collagen nanofibers (eg. 50 to 500 nm) in native ECM [16]. The mean pore size of the esPNIPAm was 1.24 ± 1.27 µm, with distribution ranges from 1 to 8 µm and majority of the pores measuring around 1 µm, as shown in Fig. 5. The pore sizes of a nanofibrous scaffold play a crucial role in regulating cellular activities and it has been established that scaffolds with pore size less than 1 µm promote cell-surface interaction while pore size of 1 to 3 µm give rise to improved cell-cell interaction [17]. The total porosity was estimated by gravimetric method as 63.6%, where a high porosity facilitates nutrient and waste exchange within the culture media [18].

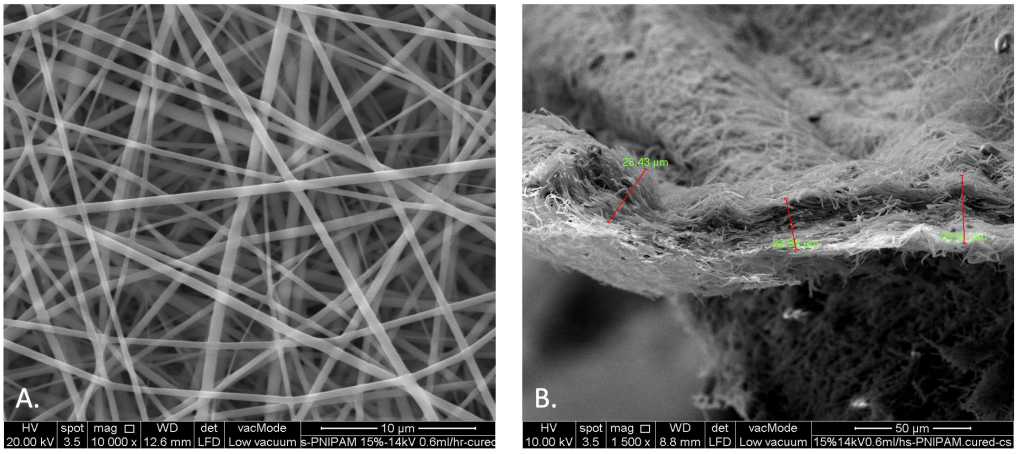

Figure 3. FESEM micrograph of (A) nanofibrous morphology and (B) cross-section of esPNIPAm.

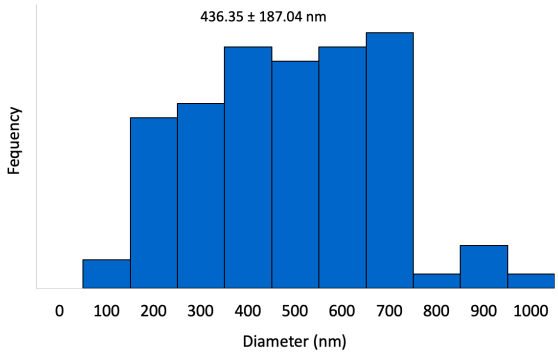

Figure 4. Fiber diameter distribution of esPNIPAm.

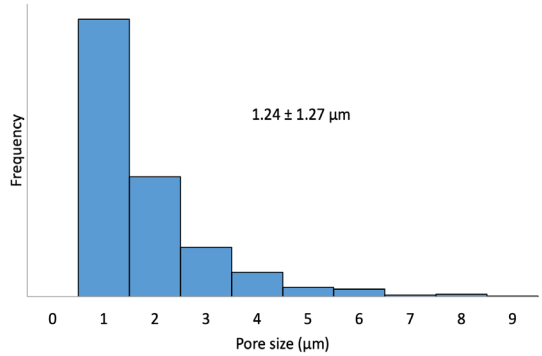

Figure 5. Pore size distribution of esPNIPAm.

Aqueous Stability of esPNIPAm. Fig. 6 shows the percentage mass loss of esPNIPAm in GMEM from day 1 through to 28. The profile shows a relatively rapid degradation rate of ~2.4 %/day from day 1 through day 7 (based on gradient of y1), amounting to 19 % mass loss. Above day 7, a much-reduced degradation rate of ~0.8 %/day can be observed (based on gradient of y2). The total mass loss at day 28 was measured at 35 %. The gradual degradation of esPNIPAm can be attributed to the dissolution of loosely entangled and non-covalently cross-linked PNIPAm chains on the membrane surface.

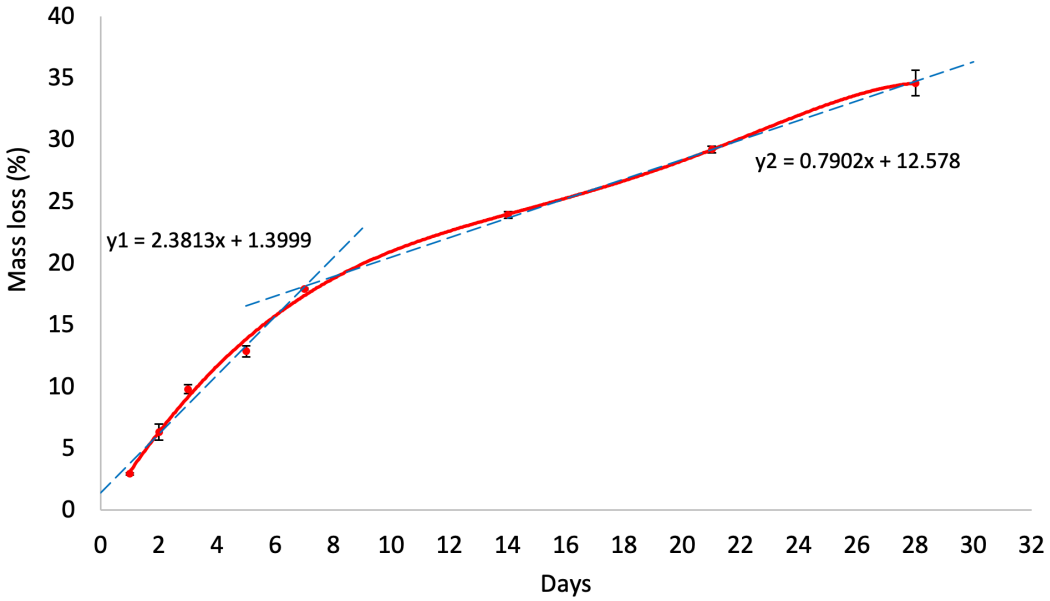

Figure 6. Percentage mass loss over time of esPNIPAm in GMEM incubated at 37 °C and 5 % CO_2.

Summary

High molecular weight neat PNIPAm synthesized via radical polymerization has been demonstrated to exhibit high electrospinnability. The resulting esPNIPAm highly mimics the native ECM in terms of fiber size and features a porous structure with porosity of 63.6 %. In addition, post electrospinning cross-linking with OpePOSS in the presence of EMI greatly improved the aqueous stability of esPNIPAm scaffold, enabling a gradual degradation in aqueous cell culture conditions with a maximum mass loss of 35 % at 28 days. This promises its feasibility as a tissue engineering scaffold by providing an initial structural support for cells as subsequent ECM is expressed.

Acknowledgement

This work was supported in part by the Department of Mechanical, Materials and Manufacturing Engineering, University of Nottingham Malaysia and Ministry of Higher Education (MOHE) Malaysia under the Fundamental Research Grant Scheme (FRGS) FRGS/1/2017/STG05/UNIM/02/1.

References

[1] A. Kramschuster and L. S. Turng, in: Handbook of Biopolymers and Biodegradable Plastics: Properties, Processing and Applications, edited by S. Ebnesajjad, chapter, 17, Elsevier Inc. (2013).

[2] F. J. O'Brien: Mater. Today Vol. 14 (2011), p. 88–95

[3] V. Capella et al.: Heliyon Vol. 5 (2019), p. e01474

[4] M. A. Cooperstein and H. E. Canavan: Langmuir Vol. 26 (2010), p. 7695–7707

[5] R. E. Young et al.: PLoS One Vol. 14 (2019), p. e0219254

[6] K. Y. Tshai, S. S. Lim, L. C. Yong, and P. M. Chou, in: Tissue Engineering Strategies for Organ Regeneration, edited by N. Sultana, S. Bandyopadhyay-Ghosh, and F. S. Chin, chapter, 3, CRC Press (2020).

[7] J. Xue, T. Wu, Y. Dai, and Y. Xia: Chem. Rev. Vol. 119 (2019), p. 5298–5415

[8] J. Wei et al.: J. Mater. Sci. Vol. 53 (2018), p. 12056–12064

[9] J. Khan, M. Siddiq, B. Akram, and M. A. Ashraf: Arab. J. Chem. Vol. 11 (2018), p. 897–909

[10] R. Contreras-Ca, L. Schellkopf, C. Ferna, I. Pastoriza-Santos, J. Pe, and M. Stamm: Langmuir Vol. 31 (2014), p. 1142–1149

[11] A. K. Tucker and M. J. Stevens: Macromolecules Vol. 45 (2012), p. 6697–6703

[12] E. H. N. Yong, K. Y. Tshai, I. C. C. Lim, S. S. Lim, Y. A. Nor, and Y. Z. H. Y. Hashim: Natl. Electrospinning Conf. 2018 (2018),

[13] J. Wang, A. Sutti, X. Wang, and T. Lin: Soft Matter Vol. 7 (2011), p. 4364–4369

[14] B. Sun, Y. Lin, and P. Wu: Appl. Spectrosc. Vol. 61 (2007), p. 765–771

[15] A. George and W. W. Wilson: Acta Crystallogr. Sect. D Biol. Crystallogr. Vol. 50 (1994), p. 361–365

[16] S. Bancelin et al.: Nat. Commun. Vol. 5 (2014), p. 1–8

[17] I. Bružauskaitė, D. Bironaitė, E. Bagdonas, and E. Bernotienė: Cytotechnology Vol. 68 (2016), p. 355–369

[18] Q. L. Loh and C. Choong: Tissue Eng. - Part B Rev. Vol. 19 (2013), p. 485–502